Time reversal in random media

Emile Mathieu
Department of Computer Science
Ecole Nationale des Ponts et Chaussees
emile.mathieu@eleves.enpc.fr

Xi Shen
Department of Computer Science
Ecole Nationale des Ponts et Chaussees
xi.shenxi@eleves.enpc.fr

Abstract

Time reversal is a technique for focusing waves and therefore imaging a source. It appears in [1] that this method can be enhanced when waves propagate in a randomly heterogeneous medium instead of a homogeneous medium. This assertion is empirically highlighted in this report by simulating waves via the paraxial wave equation.

1 Introduction

A time-reversal experiment is based on the use of a special device called time-reversal mirror. This device is an array of transducers that can be both used as sources and as receivers. In such an experiment, the time-reversal mirror is used first as a receiver array, and then as a source array.

Originally, time-reversal was proposed for energy focusing, but was then used for imaging. Indeed, time reversal of waves results in a refocusing at the original source location.

This project, aims to show that time reversal refocusing can be enhanced when the waves propagate in a randomly heterogeneous medium instead of an homogeneous medium by modeling the random medium as Gaussian Processes integrated in the wave equation.

The report is organized as follows : in the Section 3, we give both the theoretical result and the simulation output to show that how propagation and refocusing behave in a homogeneous medium; in the Section 4, a random medium is considered and modelled as certain Gaussian Processes, we compare the simulation result to the theoretical result as well; a final conclusion closes the report in Section 5.

2 Paraxial wave equation

In three dimensions spherical coordinates, due to the paraxial hypothesis the solution of a wave equation can be approximate as :

$$A(r) = \phi(r)e^{ikz}$$

where ϕ approximately solves :

$$\nabla^2\phi + 2ik\frac{\partial\phi}{\partial z} = 0$$

with $\nabla^2 = \frac{\partial^2}{\partial x^2} + \frac{\partial^2}{\partial y^2}$ is the transverse part of the Laplacian.

In our project, we study the propagation of wave in a plan xz, so the equation becomes :

$$\partial_z\phi = \frac{i}{2k}\partial_x^2\phi \tag{1}$$

which is the Schrdinger equation.

The assumption under which the paraxial approximation is valid is that the z derivative of the amplitude function ϕ is a slowly-varying function of z:

$$\left|\frac{\partial^2 \phi}{\partial_{z^2}}\right| \ll \left|k\frac{\partial \phi}{\partial_z}\right| \tag{2}$$

3 Homogeneous medium

3.1 Propagation of time-harmonic waves

We apply the Fourier transform on x in the Equation 1, and deduce that :

$$\begin{aligned} \partial_z \hat{\phi}(z,w) &= \frac{-iw^2}{2k}\hat{\phi}(z,w) \\ \Rightarrow \hat{\phi}(z,w) &= C(w)e^{\frac{-iw^2}{2k}z} \end{aligned} \tag{3}$$

Where in the Equation 3, C(w) is a function only depends on w. Since at z = 0, $\phi(0,x) = \phi_0(x)$, we obtain :

$$\begin{aligned} C(w) &= \hat{\phi}(0,w) \\ \Rightarrow C(w) &= \hat{\phi}_0(w) \\ \Rightarrow \hat{\phi}(z,w) &= \hat{\phi}_0(w)e^{\frac{-iw^2}{2k}z} \\ \Rightarrow \phi(z,x) &= \mathfrak{F}^{-1}(\hat{\phi}_0(w)e^{\frac{-iw^2}{2k}z})(z,x) \end{aligned} \tag{4}$$

Where $\hat{\phi}_0(w)$ is the Fourier transform of the initial condition $\phi_0(x) = e^{-\frac{x^2}{r_0^2}}$.

3.1.1 Analytical solution

Since the Equation 5 below,

$$\begin{aligned} \mathfrak{F}(e^{-ax^2})(w) &= \sqrt{\frac{\pi}{a}}e^{-\frac{w^2}{4a}} \\ \Rightarrow \sqrt{\frac{a}{\pi}}\mathfrak{F}(e^{-ax^2})(w) &= e^{-\frac{w^2}{4a}} \end{aligned} \tag{5}$$

With a = $\frac{1}{r_0^2}$We can obtain that :

$$\hat{\phi}_0(w) = \sqrt{\pi r_0^2}e^{-4r_0^2w^2}$$

Denote a new constant q as :

$$\begin{aligned} q &= \frac{1}{4(\frac{r_0^2}{4} + \frac{iz}{2k})} \\ &= \frac{1}{r_0^2 + \frac{2iz}{k}} \end{aligned} \tag{6}$$

With the Equation 5, the Equation 4 becomes :

$$\begin{aligned}\phi(z,x) &= \mathfrak{F}^{-1}(\sqrt{\pi r_0^2}e^{-\frac{w^2}{4q}})(z,x) \\ &= \sqrt{\pi r_0^2}\sqrt{\frac{q}{\pi}}e^{-qx^2} \\ &= \sqrt{qr_0^2}e^{-qx^2} \end{aligned} \tag{7}$$

When z = L, q = $\frac{1}{r_t^2}$, as a result, we obtain the desired solution on z = L as :

$$\phi_t(x) = \frac{r_0}{r_t}e^{-\frac{x^2}{r_t^2}}$$

3.1.2 Simulation

With the Equation 4, we can simulate the solution by Fourier transform, What we do is simply calculate the Fourier transform of ϕ_0 by fft in matlab, then we can compute the product between $\hat{\phi}_0$ and $e^{\frac{-iw^2}{2k}z}$ by taking z = L, finally we compute the inverse Fourier transform of the obtained term, which gives us the final resolution on z = L.

The simulation result is shown in the 1 as well as the theoretical result, which shows that the simulation solution is the same to the theoretical one.

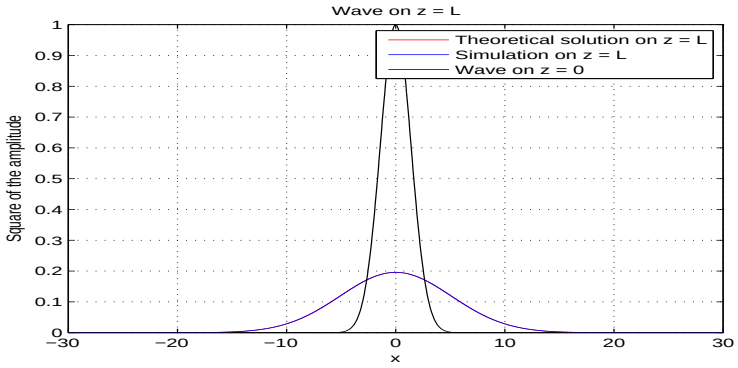

Figure 1: Propagation of time-harmonic waves, simulation with fft (blue), theoretical result (red), original wave on z = 0 (black)

3.2 Time reversal for time-harmonic waves

We have exactly the same solution as indicated in the Equation 3 but with different initial condition on x = L.

$$\begin{aligned}\hat{\phi}_{tr}(L,w) &= \mathfrak{F}(\overline{\phi_t}\chi_M)(w) \\ \Rightarrow C(w) &= \mathfrak{F}(\overline{\phi_t}\chi_M)(w)e^{\frac{iw^2}{2k}L} \\ \Rightarrow \phi_{tr}(z,x) &= \mathfrak{F}^{-1}(\mathfrak{F}[\overline{\phi_t}\chi_M]e^{\frac{iw^2(L-z)}{2k}}) \end{aligned} \tag{8}$$

Where $\overline{\phi_t(x)}$, the conjugate complex of the solution in the Section 3.1.

3.2.1 When $\chi_M(x) = [1-(\frac{x}{2r_M})^2]^2\mathbb{1}_{[-2r_M,2r_M]}(x)$

We proceed simulations for different r_M (varies from 2 to 22). The result is shown in the Figure 2.

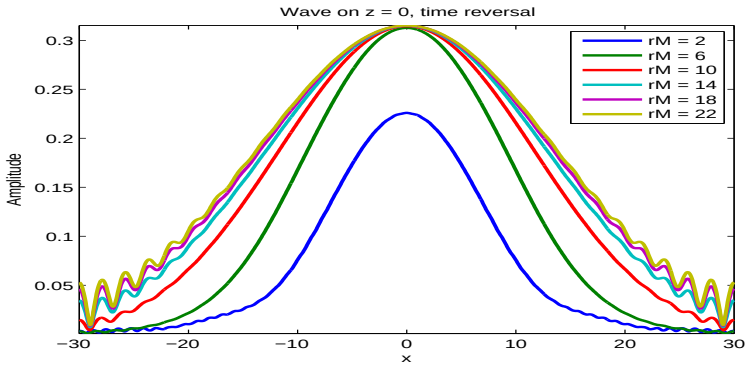

Figure 2: Time reversal for time-harmonic waves with different r_M

From the Figure 2, we notice that the refocusing becomes poor (the variance becomes big) when r_M, the radius of the mirror, gets small.

3.2.2 When $\chi_M(x) = e^{-\frac{x^2}{r_M^2}}$

Theoretical result

We proceed the same procedure as in the Section 3.1,

$$\overline{\phi_t}\chi_M = \frac{r_0}{\overline{r}_t} e^{-x^2(\frac{1}{\overline{r}_t^2}+\frac{1}{r_M^2})}$$

With $a_0 = \frac{1}{\overline{r}_t^2} + \frac{1}{r_M^2}$, we obtain the Fourier transform of $\overline{\phi_t}\chi_M$,

$$\mathfrak{F}[\overline{\phi_t}\chi_M](w) = \frac{r_0}{\overline{r}_t}\sqrt{\frac{\pi}{a_0}} e^{-\frac{w^2}{4a_0}}$$

$$\mathfrak{F}[\overline{\phi_t}\chi_M]e^{\frac{iw^2(L-z)}{2k}} = \frac{r_0}{\overline{r}_t}\sqrt{\frac{\pi}{a_0}} e^{-w^2(\frac{1}{4a_0}+\frac{i(z-L)}{2k})}$$

By the Equation 5, denotes $\frac{1}{4a} = \frac{1}{4a_0} + \frac{i(z-L)}{2k}$, then $a = \frac{1}{\frac{1}{a_0}+\frac{2i(z-L)}{k}}$, as a result, the inverse Fourier transform of $\mathfrak{F}[\overline{\phi_t}\chi_M]e^{\frac{iw^2(L-z)}{2k}}$ is finally can be computed as :

$$\begin{aligned}
\mathfrak{F}^{-1}(\mathfrak{F}[\overline{\phi_t}\chi_M]e^{\frac{iw^2(L-z)}{2k}}) &= \frac{r_0}{\overline{r}_t}\sqrt{\frac{\pi}{a_0}}\sqrt{\frac{a}{\pi}} e^{-ax^2} \\
&= \frac{r_0}{\overline{r}_t}\frac{1}{\sqrt{1+\frac{2ia_0(z-L)}{k}}} e^{-\frac{x^2}{\frac{1}{a_0}+\frac{2i(z-L)}{k}}} \\
&= \frac{1}{\sqrt{(1+\frac{2ia_0(z-L)}{k})(\frac{\overline{r}_t}{r_0})^2}} e^{-\frac{x^2}{(\frac{1}{\overline{r}_t^2}+\frac{1}{r_M^2})^{-1}+\frac{2i(z-L)}{k}}}
\end{aligned}$$

We can thus compute a_{tr} and r_{tr} on z = 0,

$$
\begin{aligned}
\frac{1}{a_{tr}} &= \frac{1}{\sqrt{(1+\frac{2ia_0(z-L)}{k})(\frac{\overline{r}_t}{r_0})^2}} \\
&= \frac{1}{\sqrt{(\frac{\overline{r}_t}{r_0})^2 - (\frac{\overline{r}_t}{r_0})^2 \frac{2ia_0 L}{k}}} \\
&= \frac{1}{\sqrt{1 - \frac{2iL}{kr_0^2} - \frac{2iL}{kr_0^2}(1+\frac{\overline{r}_t^2}{r_M^2})}} \\
&= \frac{1}{\sqrt{1 - \frac{2iL}{kr_0^2} - \frac{2iL}{kr_0^2}(1+\frac{r_0^2 - \frac{2iL}{k}}{r_M^2})}} \\
&= \frac{1}{\sqrt{1 - \frac{4iL}{kr_0^2} - \frac{2iL}{kr_M^2} - \frac{4L^2}{k^2 r_0^2 r_M^2}}}
\end{aligned} \tag{9}
$$

$$
r_{tr}^2 = (\frac{1}{r_M^2} + \frac{1}{r_0^2 - \frac{2iL}{k}})^{-1} - \frac{2iL}{k} \tag{10}
$$

Simulation result

The simulation result can be seen in the Figure 3, which present the module of the theoretical result and the module of simulation output with fft. We conclude that analytical result is verified by the simulation.

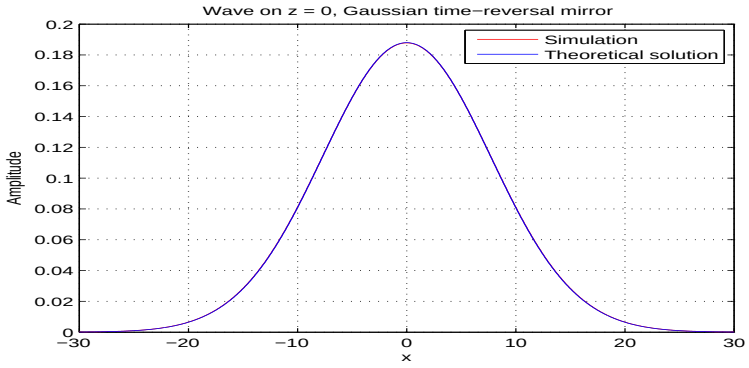

Figure 3: Time reversal for time-harmonic waves with $r_M = 2$, simulation with fft (red), theoretical result (blue)

4 Random medium

We now consider a random medium modelled by Gaussian processes (GPs). Indeed, the Schrodinger equation modelling our waves propagation is now

$$
\partial_z \phi(z,x) = \frac{i}{2k}\partial_x^2 \phi(z,x) + \frac{i}{2k}\mu(z,x)\phi(z,x) \tag{11}
$$

where μ is a potential of the form

$$
\mu(z,x) = \mu_n(x) \text{ if } z \in [nz_c n(n+1)z_c] \tag{12}
$$

$$
\text{with} \quad \mu_0(x), \mu_1(x), \ldots, \mu_{[L/z_c]}(x) \text{ independent realizations of a GP} \tag{13}
$$

4.1 Propagation of time-harmonic waves

So as to solve numerically this equation, we implement a split-step Fourier method (SSFM). The approach followed by SSFM follows the old age strategy of divide and conquer. The PDE is divided into related sub-problems of the original equation.

Here the Shrodinger equation is splitted in two parts, which are alternately and iteratively solved. First we consider

$$\partial_z \phi = \frac{ik}{2} \partial_x^2 \phi \tag{14}$$

which can be easily solved in the Fourier domain. We get

$$\mathcal{F}(\partial_z \phi) = \partial_z \mathcal{F}(\phi) = \frac{i}{2k} \mathcal{F}(\partial_x^2 \phi) = \frac{i}{2k} \times (2\pi i f)^2 \mathcal{F}(\phi) \tag{15}$$

Thus

$$\phi(z+h, x) = \mathcal{F}^{-1}(\exp\{-h \frac{i}{2k} (2\pi i f)^2\} \mathcal{F}(\phi(z, x))) \tag{16}$$

The other part of the equation is the one with the Laplacian term:

$$\partial_z \phi = \frac{ik}{2} \mu_n(x) \phi \tag{17}$$

which is an ODE and is therefore easily solved:

$$\phi(z+h, x) = \exp\{h \frac{ik}{2} \mu_n(x)\} \phi(z, x) \tag{18}$$

Hence these two steps 16 and 18 can be summed up as:

$$\phi(z+h, x) = \exp\{h \frac{ik}{2} \mu_n(x)\} \mathcal{F}^{-1}(\exp\{-h \frac{i}{2k} (2\pi i f)^2\} \mathcal{F}(\phi(z, x))) \tag{19}$$

These operations are repeated until the position in z is reached. This method is implemented in the MATLAB function `split_step_fourier_method.m`.

Since the Gaussian processes are stationary, they are sampled using the Fourier algorithm (because it is very fast), implemented in the MATLAB function `sample_GP.m`.

A total of 300 Gaussian processes are sampled, and as many forward wave propagations by SSFM are computed in each medium. The transmitted wave profile $\phi_t(x, z = L)$ is then averaged on these 300 runs. Figure 4 both shows the empirical and theoretical mean transmitted wave profile. It can be noticed that the empirical average is quite close to the theoretical expectation.

4.2 Time reversal for time-harmonic waves

We consider a Gaussian time-reversal mirror in the plane $z = L$. In this section, we perform a time-reversal experiment by backpropagating the time-reversed wave ϕ_t in the same random medium as for the propagation. Then we can compute the refocused wave $\phi_{tr}(z, x)$ in the plane $z = 0$.

For comparison purposes, we also perform the same backpropagation but in an homogeneous medium.

Those computations are again done using the split-step Fourier method, but using a negative spatial step $-h$. As in the previous part, results are averaged on 300 runs.

Figure 5 shows the mean refocused wave profile with a backpropagation performed in a random and also in an homogeneous medium, for two different values of the Gaussian mirror radius. It can be observed empirically that the variance of the refocused wave is smaller for the random medium than for the homogeneous medium.

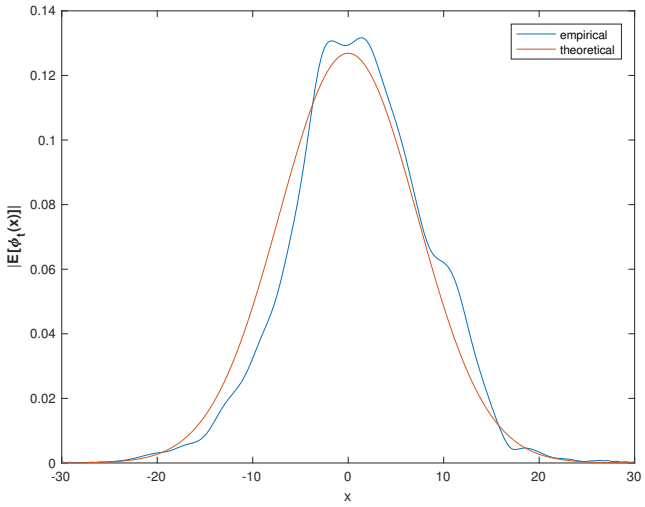

Figure 4: Mean transmitted wave profile $|\phi_t(x, z = L)|$ in random medium

This is also intelligible on a theoretical point of view given that mean refocused wave profile for a random medium is

$$\mathbb{E}[\phi_r^{tr}(x)] = \frac{1}{a_{tr}} \exp(-\frac{x^2}{x_{tr}^2}) \exp(-\frac{x^2}{x_a^2}) \tag{20}$$

whereas for a backpropagation in an homogeneous medium it is

$$\mathbb{E}[\phi_r^{tr}(x)] = \frac{1}{a_{tr}} \exp(-\frac{x^2}{x_{tr}^2}) \exp(-\frac{\gamma_0 \omega^2 L}{8}) \tag{21}$$

Since there is another Gaussian term in the mean refocused wave profile for the backpropagation in a random medium, the latter shall therefore be more peaked than the one backpropagated in a homogeneous medium.

Moreover, the larger is the Gaussian mirror radius, the smaller is the difference between the mean refocused wave profile variances (between heterogeneous and homogeneous) as it appears on Figure 5.

Indeed, since $x_{tr}^2 = \left(\frac{1}{r_M^2} + \frac{1}{r_0^2 - 2i\frac{L}{k}}\right)^{-1} + 2i\frac{L}{k}$ is an increasing function of r_M^2 the variance of the refocused waves should increase with r_M^2.

What is more, since $a_{tr}^2 = \left(1 + \frac{4L^2}{k^2 r_0^2 r M^2} + 2i\frac{L}{k r_m^2}\right)$ is a decreasing function of r_M^2, the bigger r_M^2 is the higher is the amplitude of the refocused wave. This phenomenon can indeed be observed in Figure 5.

4.3 Time reversal for time-dependent waves

In this last part we consider a time-dependent initial condition with a flat spectrum over $[\omega_0 - B, \omega_0 + B]$ and with a Gaussian transverse profile.

So as to compute the refocused wave in this scenario, we perform a time-reversal experiment for each frequency (with a chosen discretization) and the sum the frequency components.

Figure 6 shows several realizations of this process with an initial Gaussian transverse profile of radius $r_M = 10$, along with its theoretical expectation.

We also noticed that the bigger is r_M, the more statistically stable is the refocused wave.

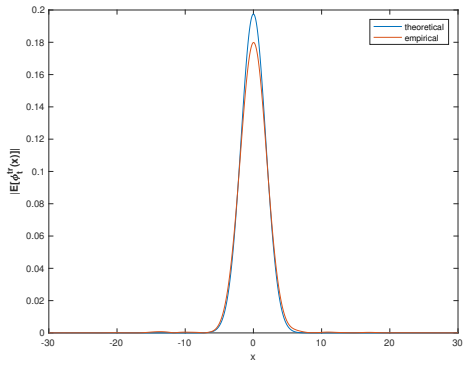

(a) Random medium with $r_M = 2$

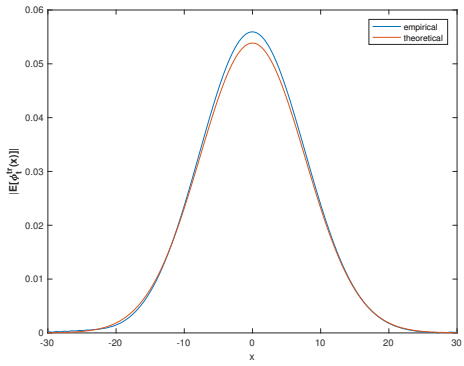

(b) Homogeneous medium with $r_M = 2$

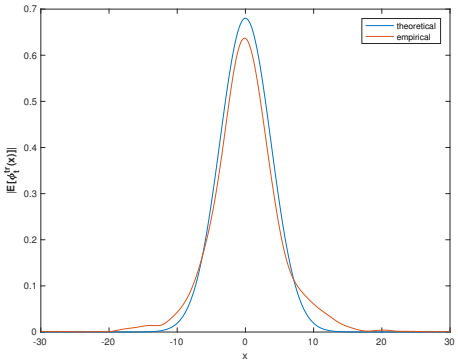

(c) Random medium with $r_M = 10$

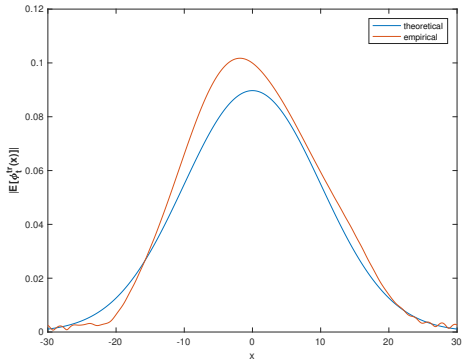

(d) Homogeneous medium with $r_M = 10$

Figure 5: Mean refocused wave profiles

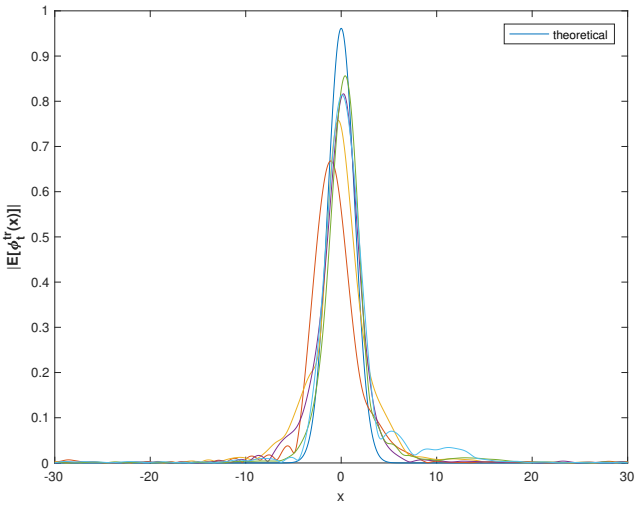

Figure 6: Several realisations of refocused wave profile for a time-dependent Gaussian initial condition with $r_M = 10$. The blue curve represents the theoretical result, and other colours shows different realisations.

5 Conclusion

We have empirically showed that propagating waves in a heterogeneous random medium instead of an homogeneous one enhances refocusing of time reversal waves.

References

[1] Peter Blomgren, George Papanicolaou, and Hongkai Zhao. Super-resolution in time-reversal acoustics. *The Journal of the Acoustical Society of America*, 111(1):230–248, 2002.